A multi-nuclear NMR study of the local structure of lead zirconate titanate, $PbZr_{1-x}Ti_xO_3$

2005 J. Phys.: Condens. Matter 17 7159

(http://iopscience.iop.org/0953-8984/17/44/009)

INSTITUTE OF PHYSICS PUBLISHING JOURNAL OF PHYSICS: CONDENSED MATTER

J. Phys.: Condens. Matter **17** (2005) 7159–7168 doi:10.1088/0953-8984/17/44/009

A multi-nuclear NMR study of the local structure of lead zirconate titanate, $PbZr_{1-x}Ti_xO_3$

A Baldwin, P A Thomas and R Dupree

Department of Physics, University of Warwick, Coventry CV4 7AL, UK

Received 14 July 2005
Published 18 October 2005
Online at stacks.iop.org/JPhysCM/17/7159

Abstract

Samples of lead zirconium titanate, $PbZr_{1-x}Ti_xO_3$ (PZT), having $x = 0$, 0.25, 0.48, 0.55, 0.75 and 1, were studied by ^{17}O, ^{207}Pb and $^{47,49}Ti$ solid-state NMR. All oxygen sites are clearly resolved for the end-member compositions and are assigned on the basis of line intensity and the correlation of the oxygen shift with increasing Zr/Ti–O bond length. The two distinct O sites characteristic of the end member $PbTiO_3$ ($x = 1$) behave differently as x is decreased, indicating that Ti–O–Ti chains in the (001) plane are preserved down to $x = 0.25$. By contrast, the Ti–O–Ti signal in the [001] direction is absent at $x \leqslant 0.75$, which demonstrates there is an important anisotropy in the local structure of PZT solid solutions. A sharp line consistent with a new well ordered oxygen environment appears at the morphotropic boundary (MPB) composition, $x = 0.48$, and is suggested to be a feature of the monoclinic phase. Although a small amount of lead is in a relatively ordered environment, there is considerable Pb disorder throughout the composition range. The ^{207}Pb shift dispersion implies a Pb–O distance variation of ∼0.02 Å for $x = 0.10$, and still larger for other compositions. The intrinsic width of the $^{47,49}Ti$ lines is found to remain constant for x values between 0 and 0.50, which indicates that the electric field gradient and the octahedral distortion observed in the $PbTiO_3$ end-member is little changed even in the presence of considerable Zr doping. These observations are discussed in the context of present models for the development of the average and local structures of PZT solid solutions throughout the phase diagram and across the MPB.

1. Introduction

Lead zirconate titanate, $PbZr_{1-x}Ti_xO_3$ (PZT), is well known as a technologically important piezoelectric material and is the current industrial standard to which new materials are compared. PZT is formed from a solid solution between $PbTiO_3$ (PT), which is described by tetragonal $P4mm$ symmetry at room temperature and is considered a classical exemplar of a perovskite ferroelectric crystal, and $PbZrO_3$ (PZ), which is described by orthorhombic space group $Pbam$ and is antiferroelectric at room temperature. The basic phase diagram for

the PZT solid solution was established more than 50 years ago (Shirane and Takeda 1952) and shows an almost vertical morphotropic phase boundary (MPB) between a rhombohedral (R) phase for $x < 0.47$ and a tetragonal (T) phase for $x > 0.47$. It was observed that the piezoelectric properties achieved a maximum in the vicinity of the MPB (Jaffe *et al* 1954, 1955), and considerable effort was devoted to explaining this phenomenon. For many years, it was believed that the transition from R to T with increasing x was achieved *via* a region of phase coexistence, an explanation consistent with the fact that the R–T phase transition is not subgroup/super-group related, thus necessitating a large degree of structural rearrangement at the phase boundary. However, in 1999, Noheda *et al* observed the existence of a distinct monoclinic phase (denoted by M_A in the terminology of Vanderbilt and Cohen 2001) of symmetry Cm at the MPB composition. Since Cm is a subgroup of both $R3m$ and $P4mm$, a phase of this symmetry conveniently bridges the otherwise unrelated R and T phases. Furthermore, by invoking a mechanism of so-called 'polarization rotation' in the monoclinic phase, it was possible to explain the large piezoelectric coefficients that appear at the MPB (Bellaiche *et al* 2000).

Whilst the existence of the M_A bridging phase is now accepted, there still remains controversy over some aspects of the PZT phase diagram. For example, Kisi *et al* (2003) have pointed out that there remains an inconsistency between the symmetry aspects of the proposed R–M_A transition and the present theoretical treatment. On the macroscopic scale, the $R3m$–Cm transition has to be first order whereas the associated physical properties are treated as varying continuously within current models. Furthermore, as pointed out first by Corker *et al* (1998), there is static or dynamic disorder, which is registered by anomalous thermal displacement parameters of the Pb atoms on the R side of the phase boundary, an aspect of the structure that the models for the transition at the MPB and for the enhanced piezoactivity observed in the vicinity have ignored. The disorder on the Pb site modelled by Corker *et al* places the Pb atoms in local environments of monoclinic symmetry within the average structure of rhombohedral (R) crystallographic symmetry. As discussed in detail in Glazer *et al* (2005), the disordered rhombohedral phase with local monoclinic displacements of the Pb atoms is a direct precursor of the ordered M_A structure found at the MPB by Noheda *et al* (1999). Furthermore, Glazer *et al* show that it is possible to view the whole sequence of R to M_A to T phases in the PZT diagram on the local scale as the growth and diminution of regions of monoclinic symmetry, thus providing a different interpretation of the notion of the phase boundary in this system. The concentration on the *local* environment of the atoms (the local structure) in addition to the long-range crystallographic (average) structure that is yielded by a conventional x-ray or neutron diffraction experiments is a particular feature of the model by Glazer *et al*. Experimental evidence was provided by diffuse scattering images in electron diffraction, which were interpreted as evidence of displacement disorder of the Pb atoms. Indeed, Glazer *et al* concentrated almost exclusively on the role of Pb disorder in their discussion of the PZT diagram, commenting that little information or discussion to date has addressed the question of order or disorder on either the shared Ti/Zr octahedral site or the oxygen sites.

Evidently, understanding the phase diagram at the local level is aided by the use of structural probes that are sensitive to the appropriate spatial scale. Solid-state NMR provides an atom-specific means of investigating the chemical environment of atoms on the scale of the chemical bond. The technique is applicable to substances from the amorphous to the highly crystalline and is well adapted to powdered samples, such as PZT. With this in mind, we report a first solid-state study of the PZT solid-solution series as a function of x across the phase diagram utilizing ^{17}O, $^{47,49}Ti$ and ^{207}Pb NMR to probe the local structure as a function of composition.

2. Experimental details

2.1. Sample preparation

PZT samples with $x = 0$, 0.25, 0.48, 0.55, 0.75 and 1 were prepared in ^{17}O-enriched form by the calcination of ^{17}O-enriched TiO_2, PbO and ^{17}O-enriched ZrO_2 for 8 h at 800 °C. The ^{17}O enrichment was achieved by first preparing the required amounts of titania and zirconia *via* a sol–gel route, and then using these oxides in the calcination step. The sol–gel process involved the hydrolysis of either titanium or zirconium iso-propoxide using 40% ^{17}O-enriched water. The sol–gel products were pumped on for several hours in order to produce a fine white powder, heat treated at approximately 110 °C for 4 h, and then washed with deionized water to remove any organic contaminants left over from the hydrolysis reaction. Care was taken in the preparation of the ^{17}O samples in order to minimize the exchange with atmospheric oxygen. The calcination of the enriched samples was performed in a sealed quartz tube, under reduced air pressure (approximately 1/5 atm).

The samples prepared were investigated using x-ray powder diffraction using a Bruker D5005 diffractometer and Cu Kα radiation, with an angular step of 0.05° and an acquisition time of 30 s per point, giving a total scan time of 10 h per sample. The data were compared with previously published patterns for samples of the same compositions.

2.2. NMR experiments

The ^{17}O NMR experiments were performed at 5.6, 8.45 and 14.1 T on Varian CMX Infinity spectrometers using a Doty 4 mm magic angle spinning (MAS) probe (low fields) and Varian 4 mm T3 probe (high fields). The high density of the PZT samples (e.g. $\sim$8 g cm^{-3} for $PbTiO_3$) reduced the maximum available MAS speed, because of the limitations of the materials used in the rotor construction, which are rated at 5 g cm^{-3}. MAS speeds of approximately 14 kHz were used. The spectrum of each sample was acquired at two different spinning speeds in order to isolate the isotropic lines from the many overlapping sideband patterns. The spectra were obtained using single-pulse techniques in the case of the high fields, whereas an Oldfield echo pulse sequence was necessary for the low-field acquisition, because of the longer spectrometer dead-time associated with the lower frequency of operation. Recycle times of between 1 and 4 s were used. All spectra were referenced with respect to tap water at 0 ppm.

The ^{207}Pb NMR was performed using a Varian CMX Infinity spectrometer, operated at a field of 4.67 T, with a 4 mm Bruker probe. The data were acquired using a rotor synchronized pulse echo sequence, with rotation rates of approximately 12 kHz and a recycle time of 5 s. The spectra were referenced to the primary standard of $Pb(CH_3)_4$ at 0 ppm, via the solid $PbNO_3$ MAS line at -3494 ppm (Fayon *et al* 1997).

The ^{47,49}Ti NMR was performed on a Varian CMX Infinity 600 using a home-built static probe. The data were acquired using an Oldfield echo pulse sequence, with the parameters optimized for the ^{49}Ti isotope (Padro *et al* 2002). The spectra were referenced to the ^{49}Ti peak of the secondary standard of $SrTiO_3$ at 0 ppm. ^{47,49}Ti MAS spectra were also obtained on the CMX600 spectrometer, using a Doty 7 mm probe. Spinning rates of 9.5 kHz were achieved by diluting the samples with SiO_2 in order to reduce the total density.

3. Results

3.1. Oxygen-17

The ^{17}O spectra of the two end members of the series is shown in figure 1. Since ^{17}O ($I = 5/2$) has a quadrupole moment, the peak position and linewidth are affected by the electric field

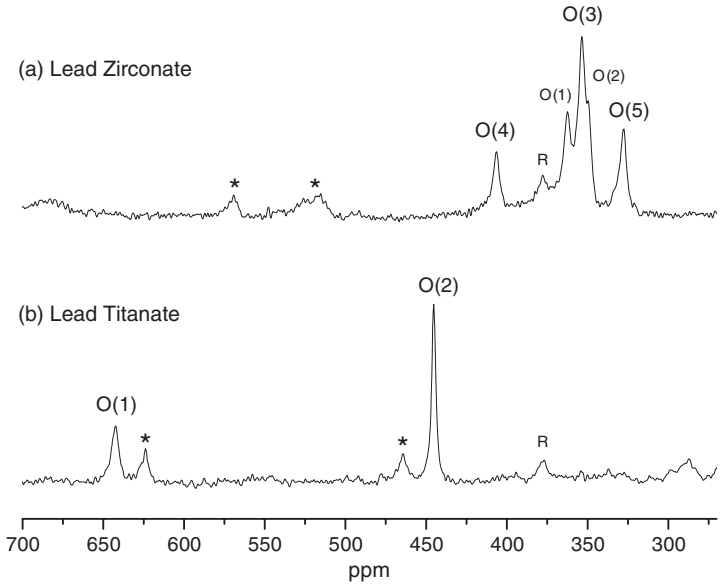

Figure 1. ^{17}O MAS NMR spectrum at 14.1 T of $PbTiO_3$ and $PbZrO_3$, the two end-members of the $PbZr_{1-x}Ti_xO_3$ solid solution. R denotes the rotor background and the spinning sidebands are marked with an asterisk.

gradient at the oxygen site. The lines in figure 1 are narrow, indicating that second-order quadrupolar broadening and, thus, the electric field gradient are small. The isotropic shift, δ_{iso}, can be obtained from the variation of the peak position, δ_{CG}, with resonance frequency ν_0 given in equation (1),

$$\delta_{CG} = \delta_{iso} - 6000 P_Q^2/\nu_0^2 \tag{1}$$

where C_Q is the quadrupole coupling constant, η the asymmetry parameter and P_Q the reduced quadrupole coupling constant, $P_Q = C_Q(1 + \eta^2/3)$. The isotropic chemical shifts and an estimate of P_Q for each of the oxygen sites in PZ and PT were extracted from a plot of δ_{CG} against $1/\nu_0^2$ for measurements performed at several different field strengths.

The lead titanate (PT) structure (Nelmes and Kuhs 1985) possesses two inequivalent oxygen sites, axial and equatorial (figure 2), which occur in the unit cell in the ratio 1:2. The spectra can be accurately simulated using two Gaussian/Lorentzian lines with the intensity ratio 1:2. This assigns the line at 445 ppm to the O(2) equatorial site, and the line at 645 ppm to the O(1) axial site. The measured P_Q values (table 1) are in good agreement with the values calculated *ab initio* (Baldwin 2003, Jennings 2004) using the WIEN2000 code. The good agreement between experiment and theory (it is typically better than 10% for WIEN calculations of P_Q (Padro *et al* 2002)) is indicative of the quality of the data and provides confidence in our interpretation of the NMR spectra.

The lead zirconate (PZ) structure (Corker *et al* 1997) possesses five inequivalent oxygen sites, which occur in the ratio 1:1:2:1:1 within the unit cell. The spectra can be simulated using five Gaussian/Lorentzian lines, with integrated intensities in the ratio 0.9:1.3:2:0.8:1, which is close to the expected result. It is somewhat more difficult to assign each of the lines to the oxygen sites than for the case of lead titanate. The line that occurs with twice the integrated intensity of the other four can be immediately assigned to the site that occurs twice in the asymmetric unit, labelled O(3) in this case. The other four sites are assigned on the basis of

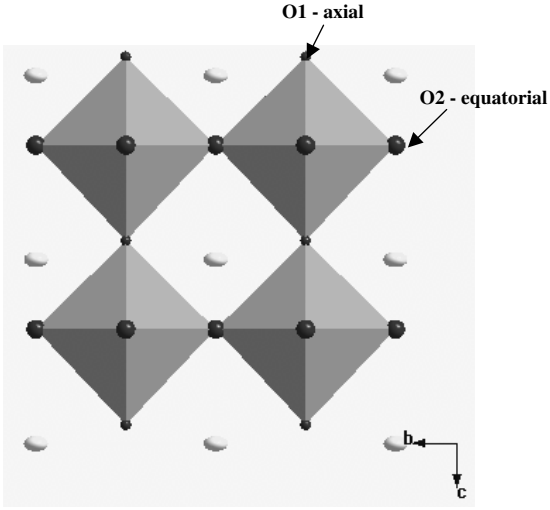

Figure 2. A representation of one unit cell of the crystal structure of $PbTiO_3$ viewed along the [100] direction. The Pb atoms are represented by thermal ellipsoids at the 50% probability level and the shaded octahedra enclose the Ti atoms (not shown). The dark spheres represent the oxygen atoms at the vertices of the octahedra with the axial (O1) and equatorial (O2) positions indicated.

Table 1. The ^{17}O NMR parameters and O–M (M = Ti, Zr) bond lengths of lead titanate and lead zirconate.

Sample	Site	$_{iso}$ (ppm)	P_Q (MHz) Expt	P_Q (MHz) Calc	Bond length (Å)
$PbTiO_3$	O(1)	647(±2)	<0.5	0.35	2.112(5)
	O(2)	443(±2)	0.9(±0.3)	0.88	2.094(5)
$PbZrO_3$	O(1)	365(±2)	1.0(±0.3)		2.098(5)
	O(2)	351(±2)	1.0(±0.4)		2.111(5)
	O(3)	356(±2)	1.0(±0.3)		2.047(8)
					2.205(8)
	O(4)	408(±2)	0.8(±0.2)		2.142(3)
	O(5)	329(±2)	0.8(±0.2)		2.044(2)

the O–Zr bond lengths, assuming that the proximity of the Zr ion plays the most important shielding role. The two outer lines are well separated from the other three, and can be assigned to the oxygen sites with the longest and shortest O–Zr bond lengths, O(4) at 408 ppm and O(5) at 329 ppm. The final two peaks, at 365 and 351 ppm, are assigned to O(1) and O(2) respectively. The ^{17}O NMR parameters for the end members of the PZT series are summarized in table 1.

The full range of the ^{17}O data for the PZT series is shown in figure 3, along with the two end members for comparison and the observed structural phases determined from the XRD analysis (indicated on the right-hand side). As the Zr content increases the O(1) line quickly decreases in intensity, and can no longer be observed in the PZT055 sample. Two broad features appear around 360 and 430 ppm. The intensity of the peak at 430 ppm gradually increases as the Zr content increases, up until ∼55 at.% Zr. As the Zr content increases above 55 at.%, the intensity decreases, until this line is no longer visible for the PZT025 sample. The peak at 360 ppm first becomes visible in the PZT055 sample, and its intensity increases with increasing Zr content, reaching its maximum in the PZT025 sample. The most surprising

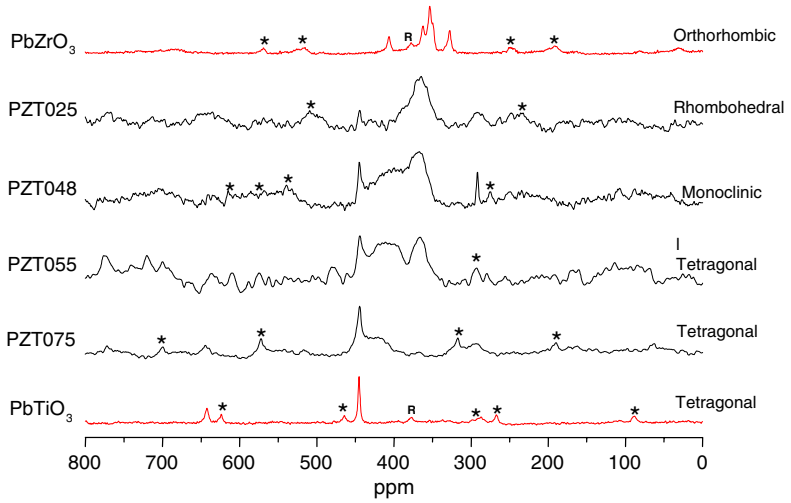

Figure 3. ^{17}O NMR of the PZT Series at 14.1 T. Spinning sidebands are marked with an asterisk. (This figure is in colour only in the electronic version)

feature of the ^{17}O data is the presence of a sharp line (of width $\Delta\nu \sim 2.5$ ppm) at 287 ppm. On close inspection of the data from the other compositions, it is clear that this line is also evident, although less sharp, in the PZT055 and PZT025 samples.

No impurity lines are visible from either anatase or rutile (at positions of 551 and 591 ppm respectively) in any of the PZT samples. This is confirmed by the XRD patterns for each composition. Any contamination by zirconia would be especially problematic, as it would overlap with the genuine signal from the PZT ceramics in an already complicated region of the spectrum. There are two likely forms of this impurity, monoclinic zirconia with peaks at 404 and 322 ppm (arising from any unreacted ZrO_2 present), and stabilized tetragonal zirconia with a single peak at 378 ppm (commonly used in MAS rotors). This background peak is visible in the spectra of the two end members, as these were acquired using standard zirconia rotors. However, this does not complicate the spectral assignment, as this particular background peak is well separated from the genuine signal. The intermediate compositions were acquired using a SiN_4 rotor, which eliminates the problem of the background signal. The XRD trace displays no evidence of any unreacted ZrO_2 across the whole sample range. Thus, the features observed are believed to be genuine signals from the PZT samples.

3.1.1. Lead-207. The ^{207}Pb spectra are shown in figure 4. The isotropic shift of the two PZT end members is in agreement within error with those given by Zhao *et al* (1999), with two isotropic peaks at 1355($\pm$10) ppm and 1025($\pm$10) ppm for $PbZrO_3$ and one at 1415($\pm$10) ppm for $PbTiO_3$. The intermediate compositions, up to 75% Zr, can be described as consisting of two components, one broad and un-narrowed together with a small component with sharp MAS lines superimposed at the positions expected for unmodified lead titanate. The narrowed component of the PZT010 sample is much broader and has a greatly reduced isotropic shift of -1125 ppm.

3.1.2. Titanium-49/47. As the Zr content and the chemical (substitutional) disorder on the B site are increased, the sharply resolved signatures of the Ti spectrum in PT (figure 5) are

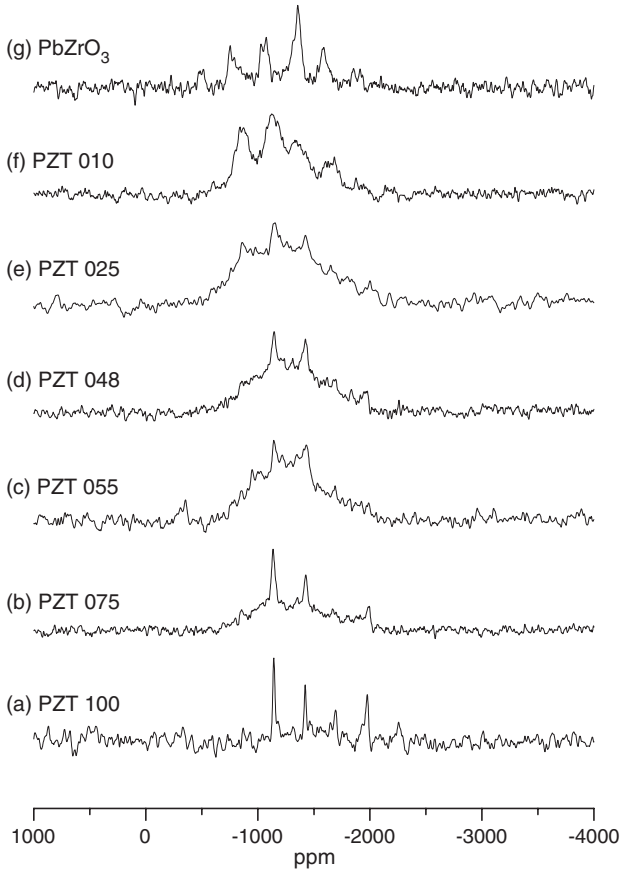

Figure 4. ^{207}Pb NMR spectra of the PZT series.

gradually smeared out, but the overall lineshape and linewidth is retained up to a Zr content of 50 at.%, which indicates that there is little change in the electric field gradient at the Ti sites.

4. Discussion

The NMR data as a function of composition provide new insight into the local structural arrangements in the PZT solid solutions, with the ^{17}O data being particularly informative. The lead zirconate structure has been the subject of many XRD and neutron diffraction experiments because of disagreement about whether or not the oxygen framework exhibits some degree of disorder. The findings of the XRD study by Corker *et al* (1997) were in favour of an ordered oxygen substructure, an argument supported by the five clearly resolved oxygen peaks observed in the ^{17}O spectrum here. The sites can be assigned on the basis that the ^{17}O shift increases with the O–Zr bond length (figure 6). The average O(3) bond length lies away from the approximately linear variation found for the other sites, probably because this site has a highly asymmetric coordination environment (Zr–O bond lengths 2.05 and 2.20 Å) and the shift is most influenced by the shortest Zr–O bond in the coordination. The other four oxygen sites each have two equidistant Zr neighbours. The lead titanate spectrum shows a far greater separation of the O(1) and O(2) oxygen lines than is observed in the closely related $BaTiO_3$

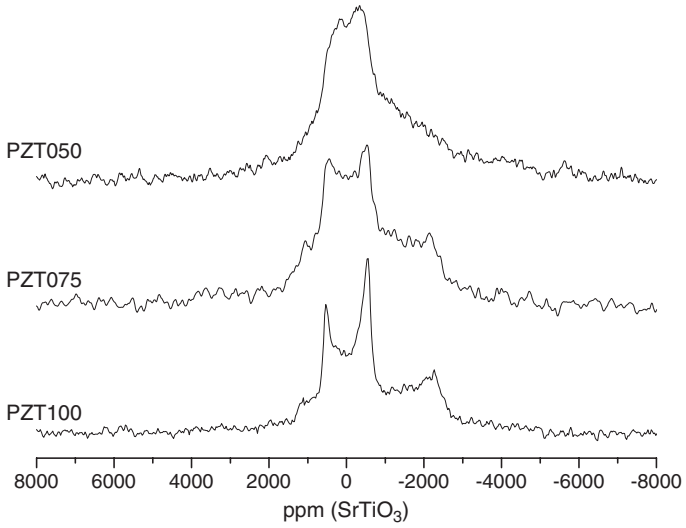

Figure 5. ^{47,49}Ti NMR spectrum at 14.1 T of the Ti rich end of the PZT series.

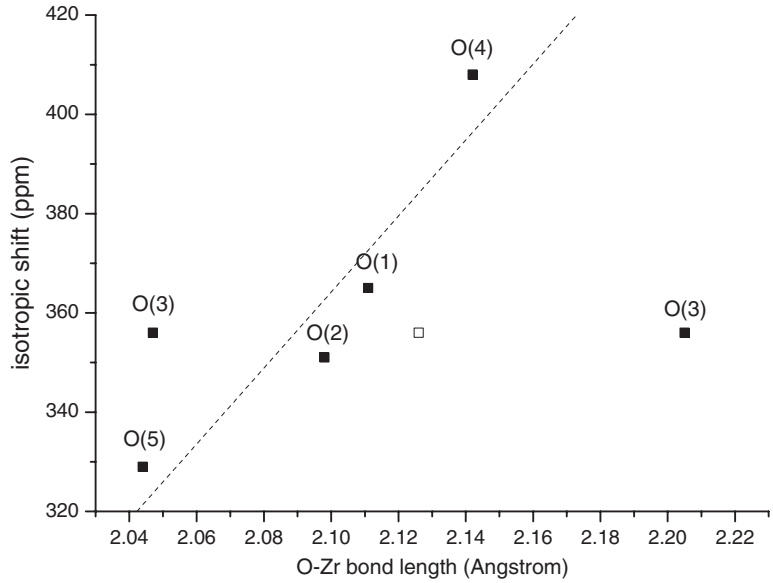

Figure 6. A graph showing the correlation of the isotropic chemical shift each of the five oxygens in $PbZrO_3$ with the O–Zr bond-length. The average of the two Zr–O3 bond-lengths is marked by the open square.

structure, a splitting of 200 ppm for PT as compared to 40 ppm for $BaTiO_3$. This is the consequence of the higher tetragonal c/a ratio of 1.06 for PT compared to 1.01 for $BaTiO_3$.

For the intermediate compositions, the ^{17}O data suggest that there is an important difference between the axial (O1) and equatorial (O2) oxygen sites as Zr is progressively added to $PbTiO_3$. The retention of the sharp line at 445 ppm, which is characteristic of the equatorial oxygen environment in PT, up to and including the Zr = 75% composition, shows

that a Ti–O2–Ti site continues to exist in Zr-rich PZT. This signifies that there is a strong tendency to retain successive Tis upon neighbouring B sites in the equatorial plane, i.e. a type of Ti 'clustering' on a spatial scale of two (at least) unit cells. By contrast, the Ti–O1–Ti signal at 645 ppm disappears rapidly. It is evident that the substitution of Zr in PT is not completely random and that there is a degree of spatial anisotropy.

Another obvious feature of the ^{17}O spectra is the new sharp line that appears at 287 ppm in the spectrum for PZT048, which is the composition corresponding to the morphotropic phase boundary. This line indicates the occurrence of a new well defined oxygen environment in the MPB material. Since the compositional steps in this preliminary study are rather coarse, it is not possible to say over what range of composition the sharp line exists. However, inspection of the data confirms that a considerably broader feature occurs at this position for the PZT025 and PZT055 compositions. It is tempting to view this line as evidence of a new oxygen environment in the distinct crystalline M_A bridging phase at the MPB. The size of the chemical shift suggests that the new environment is a Ti–O–Zr site, which becomes ordered in the crystallographic sense (i.e., is identical whenever it occurs) as the long-range order of the M_A phase is established. The site has disordered precursors, signified by the broad features at the same chemical shift in the R and T compositions either side of the boundary. The sharpness of the new oxygen peak at the MPB also implies a decrease in the degree of disorder of the Pb atom adjacent to the oxygen in question, which is consistent with a model of the M_A phase as one in which Pb displacements 'lock in' to one of three possible monoclinic displacement directions of the disordered R phase.

There is little change in the ^{17}O spectra for the oxygen assigned to the Zr–O–Zr sites between PZT048 and PZT025, in which composition interval the second-order phase change from symmetry $R3m$ to $R3c$ occurs. This phase transition is from a ferroelectric phase in which the oxygen octahedra are un-tilted to a phase in which they have equal tilts, denoted by $a^-a^-a^-$ (Glazer 1972) about the [111] axis of the pseudo-cubic unit cell. The immediate local environment of an oxygen is little changed by rotation of rigid BO_6 octahedra as the B–O interactions are hardly modified. Furthermore, in PZT there is compositional disorder on the B sites, which will dominate any small local effects produced by tilting. Although another effect of octahedral tilting is to shrink the volume surrounding the A site, thus modifying the A–O interactions, the considerable displacement disorder of the Pbs will dominate the signal both in the un-tilted and tilted phases. Therefore, it is unsurprising that the $R3c$–$R3m$ transition is not registered in the ^{17}O NMR signal.

The ^{207}Pb MAS data consist of a narrowed component, with a relatively sharp isotropic line and sidebands, along with an un-narrowed broad underlying peak due to chemical shift dispersion arising from the disorder in the lead environment. At the Zr-rich end of the phase diagram (PZT010), macroscopically the R phase, the disorder is small enough that the residual linewidth under MAS can be determined as $\sim$190 ppm. The ^{207}Pb shift has been shown to correlate quite well with mean Pb–O bond length in simple/ionic systems where the Pb–O distance is greater than 2.4 Å (Fayon *et al* 1997). If a similar correlation were applied to the perovskites, then this shift dispersion would correspond to a Pb–O distance variation of $\sim$0.02 Å, which is far greater than the typical standard deviation on a bond-length ($\sim$0.002 Å) and is, therefore, significant in indicating disorder on the Pb site. For larger concentrations of Ti, the broad component does not narrow under MAS at 12 kHz, indicating still greater disorder in the Pb–O distance. Towards the MPB, there is some narrowed component, suggesting that a small proportion of Pb is now in a well ordered environment. In the T phase, the fraction of well ordered Pb sites increases.

As Zr is introduced into PT, the two sharp $^{47,49}Ti$ lines are smeared out. However, the inherent line-widths for these components remain constant showing that the field gradient at

the Ti site remains similar to that of the end-member composition. Padro *et al* have established a strong correlation between the electric field gradient measured by NMR and the octahedral distortion parameter in titanate perovskites. The invariance of the field gradient with Zr substitution suggests that Ti-containing octahedra are relatively insensitive to the presence of ZrO_6 octahedra in the material, independently retaining the ferroelectric distortions and field gradient characteristic of the $PbTiO_3$ phase. Corker *et al* also suggested that Ti and Zr display different displacements within their octahedral environments, although determination of the sizes of these shifts was at the limit of their resolution. Their results indicated an off-centre polar displacement for Ti in agreement with these findings from NMR, and zero displacement for Zr.

5. Concluding remarks

This multi-nuclear solid-state NMR study of PZT as a function of composition is the first in this system and amply demonstrates the usefulness of this measurement technique for extracting important structural information that is inaccessible by other methods. ^{17}O NMR is seen to be a particularly useful probe of local structure in PZT as it can clearly distinguish between different sites, e.g. equatorial and axial Ti–O–Ti environments. A further more detailed multi-nuclear NMR study of the PZT solid solution, which employs finer compositional steps over the morphotropic phase boundary, is now in progress.

Acknowledgments

AB thanks EPSRC for funding a PhD studentship. The NMR equipment was partially funded by EPSRC.

References

Baldwin A J 2003 *PhD Thesis* University of Warwick
Bellaiche L, Garcia A and Vanderbilt D 2000 *Phys. Rev. Lett.* **84** 5427–30
Corker D L, Glazer A M, Dec J, Roleder K and Whatmore R 1997 *Acta Crystallogr.* B **53** 135–42
Corker D L, Glazer A M, Whatmore R W, Stallard A and Fauth F J 1998 *J. Phys.: Condens. Matter* **10** 6251–69
Fayon F, Farnan I, Bessada C, Coutures J, Massiot D and Coutures J P 1997 *J. Am. Chem. Soc.* **119** 6837–43
Glazer A M 1972 *Acta Cryst.* B **28** 3384
Glazer A M, Thomas P A, Baba-Kishi K, Pang G K H and Tai C W 2005 *Phys. Rev.* B **70** 184123–9
Jaffe B, Roth R S and Marzullo S J 1954 *J. Appl. Phys.* **25** 809–10
Jaffe B, Roth R S and Marzullo S J 1955 *J. Res. Natl Bur. Stand.* **55** 239–49
Jennings V L 2004 *PhD Thesis* University of Warwick
Kisi E H, Piltz R O, Forrester J S and Howard C J 2003 *J. Phys.: Condens. Matter* **15** 3631–40
Nelmes R J and Kuhs W F 1985 *Solid State Commun.* **54** 721
Noheda B, Cox D E, Shirane G, Gonzalo J A, Cross L E and Park S-E 1999 *Appl. Phys. Lett.* **74** 2059–61
Padro D, Jennings V, Smith M E, Hoppe R, Thomas P A and Dupree R 2002 *J. Phys. Chem.* B **106** 13176–85
Shirane G and Takeda A 1952 *J. Phys. Soc. Japan* **7** 5–11
Vanderbilt D and Cohen M H 2001 *Phys. Rev.* B **63** 094108(9)
Zhao P, Prasad S, Huang J and Shore J S 1999 *J. Phys. Chem.* B **103** 10617–26